AIAA JOURNAL
Vol. 36, No. 7, July 1998

Near Field of the Tip Vortex Behind an Oscillating Rectangular Wing

B. R. Ramaprian* and Youxin Zheng†
Washington State University, Pullman, Washington 99164-2920

Data on the evolution of the unsteady three-dimensional tip vortex in the near wake (0–3 chordlengths behind the wing) of a rectangular NACA 0015 wing oscillating sinusoidally in pitch about its quarter-chord axis are presented. These data were obtained using three-component laser Doppler velocimetry (LDV). The experiments were performed in a low-speed wind tunnel at a Reynolds number of 1.8×10^5. The wing had a semiaspect ratio of 2. It was oscillated at a frequency of 1 Hz and an amplitude of 5 deg around a mean incidence of 10 deg. The instantaneous LDV data were used to obtain information on the distribution of phase-locked velocity and vorticity components across the vortex, as well as the phase-locked circulation associated with the evolving vortex. The data indicate that the average trajectory of the oscillating vortex in the near field is very nearly the same as for a stationary wing at the mean incidence. The length and circulation scales, as well as the maximum circulation carried by the vortex flow under the conditions studied, are modulated in a significantly nonquasisteady manner. Nevertheless, beyond about 0.7 chordlength, the normalized circulation distribution across most of the inner part of the vortex exhibits, at all times, the same universal behavior as the vortex behind a stationary wing.

Nomenclature

C_L = overall lift coefficient for stationary wing at α equal to 10 deg
c = wing chord
f = frequency of oscillation
k = reduced frequency, $(\pi f c/U_\infty)$
L = reference length scale, $cC_L/2$
Re = Reynolds number, $U_\infty c/\nu$
r = radial coordinate
r_1 = radius at maximum V_θ
t = time
U = phase-locked velocity in the x direction
U_∞ = freestream velocity
V = phase-locked velocity in the inboard (y) direction
V_θ = circumferential average of v_θ
v_θ = phase-locked tangential velocity in the vortex
W = time-mean velocity in the z direction
x = distance along the freestream from the trailing-edge plane
x_v = distance along the freestream from the leading-edge plane
y = spanwise distance measured inboard from the tip
y_0 = distance inboard of the vortex center from the tip
z = direction normal to the freestream (vertically upward)
z_0 = z displacement of vortex center relative to the trailing edge
α = instantaneous angle of incidence
Γ = phase-locked circulation around a circle of radius r
Γ_1 = phase-locked circulation at radius r_1
$\Gamma_{\max}$ = circulation associated with vortex
$\Delta\alpha$ = amplitude of oscillation
ν = kinematic viscosity
ω_x = axial component of vorticity
ω_y = spanwise component of vorticity
ω_z = component of vorticity along the z direction
$\bar{}$ = time average value
$*$ = length normalized by L

Received Sept. 12, 1997; revision received March 31, 1998; accepted for publication April 1, 1998.

*Professor, School of Mechanical and Materials Engineering. Member AIAA.
†Graduate Student, School of Mechanical and Materials Engineering.

Introduction

THE study of the structure of the unsteady streamwise vortex (the so-called wing-tip vortex) in the near wake behind a rectangular wing has important practical applications, notably in helicopter rotor aerodynamics. Such data are often needed to provide the downstream boundary conditions in the computation of the rotor blade aerodynamics. Additionally, vortex-wake characterization in the near wake of a forward blade is important to describe the flow as seen by the blade advancing behind. Flow-visualization studies by Freymuth[1] and Freymuth et al.[2,3] behind stationary and pitching wings have shown that in the near-wake region, $0 < x/c < 1$, of the wing tip, the flow is characterized by the rolling up of the shear layer coming out of the trailing edge, into a spiral. The flow in this region is highly three dimensional and exhibits strong spatial velocity gradients. Some quantitative studies of flow evolution in this region for the case of a stationary wing have been reported in Refs. 4–6 and more recently by McAlister and Takahashi,[7] Ramaprian and Zheng,[8] Dacles-Mariani et al.,[9] and Chow et al.[10] Reference 8 represents a comprehensive study of the dynamics of the vortex rollup process and subsequent evolution of the vortex in the region $0 < x/c < 3$ in steady flow over a stationary wing of NACA 0015 profile. The present paper describes the next phase of this study in which the same flow region was studied with the wing oscillating sinusoidally in pitch about its quarter-chord axis. It is the expectation that the evolution of the three-dimensional unsteady vortex flowfield in the near wake in this case is a reasonable approximation to that occurring in the case of the helicopter rotor blade. To the authors' knowledge, there are no detailed quantitative data available on such unsteady flows. Thus, the present data are useful for understanding the highly vortical near wake behind the wing tip and for modeling it more accurately than has been possible in the past. All of the data obtained in this study have been archived and are available to any interested user.

Experimental Details

The experiments were conducted in the same low-speed wind tunnel of test section 1 × 1 m in cross section, using the same rectangular wing model [NACA 0015 profile of chord = 300 mm (1 ft) and semispan = 600 mm (2 ft)], as was used in the earlier stationary-wing studies of Ref. 8. In this case, however, the wing was oscillated sinusoidally in pitch about its quarter-chord ($c/4$) axis by a Scotch–Yoke mechanism driven by a speed-regulated dc motor. The oscillation conditions are given by

$$\alpha = \bar{\alpha} + \Delta\alpha \sin 2\pi f t \tag{1}$$

with $\bar{\alpha} = 10$ deg, $\Delta\alpha = 5$ deg, and $f = 1$ Hz. At the test-section velocity of about 8 m/s, the selected oscillation frequency corresponds to a reduced frequency k of approximately 0.1, which is relevant to helicopter rotor-blade dynamics. The mean Reynolds number of the flow in the tunnel was about 1.8×10^5, which is the same as in the earlier studies. No mechanical boundary-layer trip was used to promote transition. Past experience with unsteady boundary layers seems to suggest that imposed periodicity has the same effect of promoting early transition. However, no detailed studies of transition effects were performed in this investigation.

A three-color, six-beam, fiber-optic-based laser Doppler velocimetry (LDV) system, mounted on an automated three-dimensional traverse was used to obtain the three components of velocities in the flowfield within a focal volume of $0.2 \times 0.1 \times 0.1$ mm. The experimental setup is shown schematically in Fig. 1. The seeding for LDV measurements was provided by introducing fine water particles from an ultrasonic humidifier through perforations on the pressure side and the tip of the (hollow) wing model. The experimental setup and seeding details are described in detail in Ref. 8 and other earlier reports. Information on the phase angle and instantaneous direction of wing motion (viz., pitch up or pitch down) during the oscillating cycle was obtained from an optical encoder (which had a resolution of 4096 parts per revolution) mounted on the pitching axis. This was recorded simultaneously with the velocity signals from the three LDV frequency counters. The instantaneous velocities were subsequently ensemble averaged over a large number of oscillation cycles (ranging from 50 to 500) to obtain phase-locked averages of the flow properties at various phase positions during the cycle. Data corresponding to pitch-up (increasing α) and pitch-down (decreasing α) parts of the cycle were ensemble averaged separately. Measurements were made across the vortex (in the y–z plane) at several longitudinal stations in the range $0.16 < x/c < 2.66$. At each station, data were obtained at about 500 points, which formed a fine grid. The grid size and distribution were selected so as to span the region containing significant vorticity during the entire oscillation cycle and to provide a spatial resolution adequate for the evaluation of the vorticity vector. All of the experimental data have been archived and are available to any interested user. Only a typical sample from the extensive data collected will be presented and discussed here.

Phase-locked vorticity components were estimated from the phase-locked velocity data ignoring the streamwise velocity gradient. This assumption was justified from actual measurements of streamwise velocity gradients measured at $x/c = 0.33$. The expected experimental uncertainties of some key quantities are as follows: phase-locked velocities, $0.03U_\infty$; phase-locked vorticity components, 15%; phase-locked circulation, 3%; and vortex center location, $\pm 0.0015c$. A detailed discussion of several issues such as model blockage, sidewall effects, and seeding, is provided in Ref. 8, wherein it was shown that despite these usual experimental limitations, acceptably accurate results could be obtained from the present experimental arrangement.

Results

Velocity and Axial Vorticity Distributions

Figure 2 shows two sets of instantaneous contour maps of the tip vortex in the region studied. Both sets show contours of the U component of the phase-locked velocity within the vortex at the same angle of incidence of 10 deg, except that the top set corresponds to the pitch-up phase of the oscillation cycle, whereas the bottom set refers to the pitch-down phase. The difference between the two sets is quite striking and indicates that the flow exhibits a significant degree of hysteresis. Referring to the pitch-up phase, one can notice the evolution of the central core region with a significant velocity defect, from a spiral near the trailing edge to a well-formed and fairly axisymmetric configuration beyond about $x/c = 1$. A low-velocity tail, however, still persists even at the downstream end of the measurement region. This spatial evolution of the vortex takes place due to the continuous feeding of the low-velocity vortical fluid from the inboard regions of the wing wake into the spiral and the continued tightening of the turns of the spiral with distance downstream. The

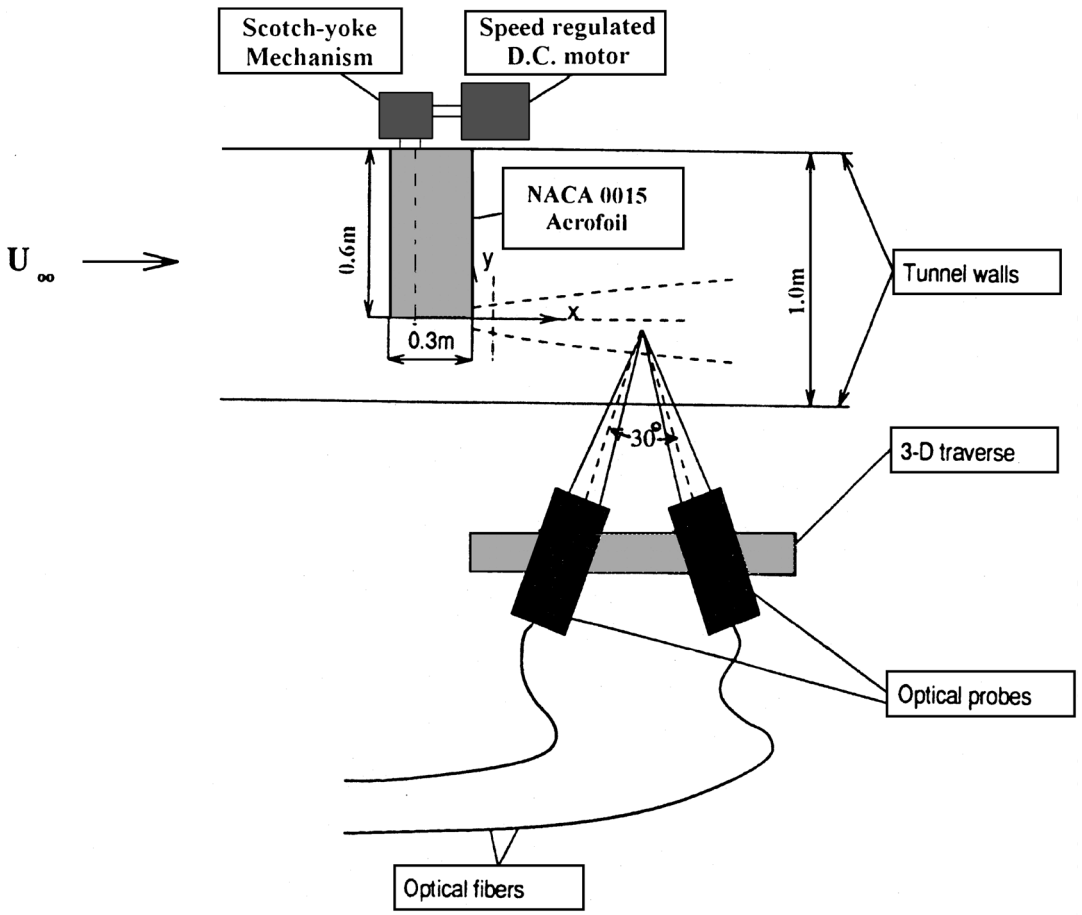

Fig. 1 Experimental setup.

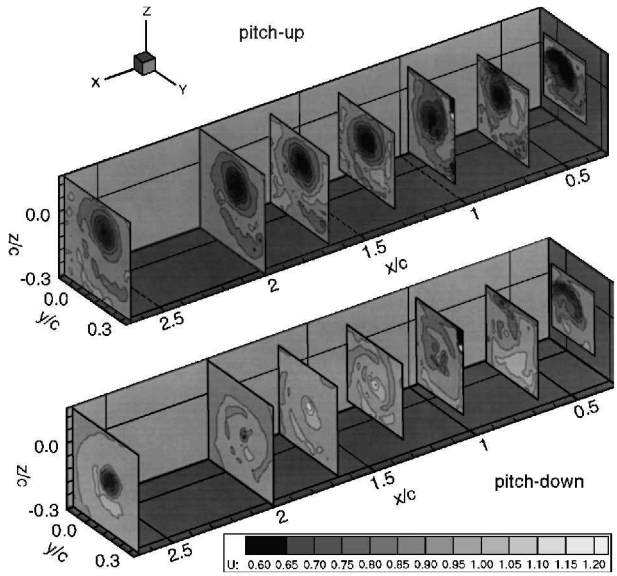

Fig. 2 Contours of the phase-locked U component of velocity in the vortex at different longitudinal locations at fixed angle of incidence of 10 deg.

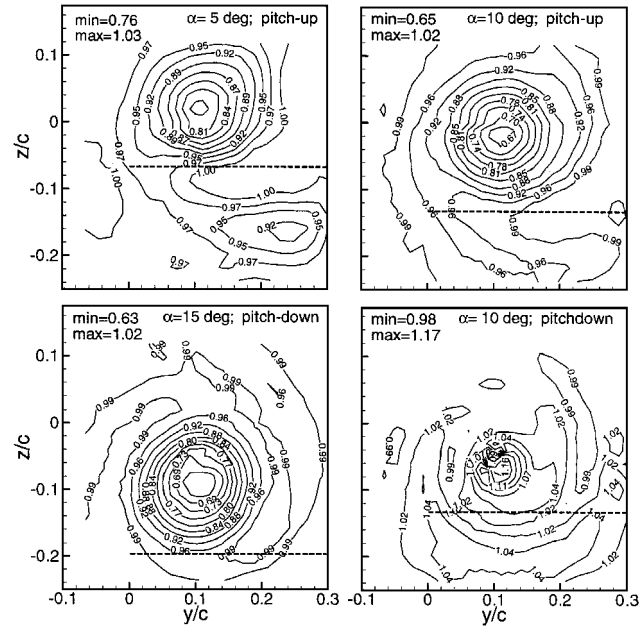

Fig. 3 Contours of nondimensional phase-locked, axial velocity U/U_∞ at different instantaneous incidences during the oscillation cycle at x/c = 1.33: Dashed line indicates the instantaneous position of the trailing edge.

qualitative nature of the flow is not unlike that observed in the tip vortex behind a stationary wing.[8,11] During the pitch-down motion, the flow is highly agitated. This agitation is mostly due to the growth and separation of the turbulent boundary layer on the suction side of the wing, which feeds into the vortex. Such flow separation during a part of the oscillation cycle was observed in preliminary flow-visualization studies. It can be seen that the velocity differences across the vortex are smaller. Indeed, velocity excesses are seen at some of the intermediate stations. However, the velocity defects reappear at the more downstream stations. These anomalies can be understood to some extent if one notes that the details seen at different longitudinal locations in the wake actually correspond to different evolution times during the convection of the vortex by the main stream. In other words, one has to account for phase shift effects in interpreting the details seen from a contourmap at a given incidence. Figure 2 suggests that beyond $x/c \cong 1.5$ the flow in a large central part of the vortex is approximately axisymmetric during the entire oscillation cycle.

Figure 3 shows the contours of the nondimensional, phase-locked U component of the velocity in the vortex at a typical fixed location, $x/c = 1.33$, and at four typical instants during the oscillation cycle. The specific instants shown are (moving clockwise through Fig. 3), $\alpha = 5$ and 10 deg during pitch up and $\alpha = 10$ and 15 deg during pitch down. In each case, the horizontal dashed line indicates the instantaneous location of the wing trailing edge. The maximum and minimum contour values are also shown. It is seen that, except at the incidence of 10 deg during pitch down, the velocity in the interior of the vortex is generally lower than in the freestream. Also, the velocity generally increases with radius in the central part of the vortex. Thus, the core region is wakelike in character. The minimum velocity occurs at the center of the core (to be defined later) and varies from $0.65U_\infty$ to $0.76U_\infty$.

Over a small part of the oscillation cycle, as typified by $\alpha = 10$ deg during pitch down, the longitudinal velocity in the vortex was found to be almost everywhere above the freestream velocity. It is seen that at $\alpha = 10$ deg, the velocity has a maximum value of $1.17U_\infty$ at the center of the vortex and generally decreases with radius. The velocity difference across the vortex, thus, is much smaller than during pitch up. This is because of the agitation and mixing already referred to. The vortex, thus, exhibits a weak jetlike behavior in this case.

Spiral layers can be easily distinguished in the contours at all of the four instants of the oscillation cycle shown in Fig. 3. These spirals correspond to the shear layer from the inboard regions of the flow, which is in a process of rolling up to form the axial tip vortex. It is also seen that the flow is approximately axisymmetric over the core region at this station, especially during the pitch-up phase. Finally, it is seen that the vortex center moves up and down but at this streamwise location remains above the trailing edge during the entire oscillation cycle.

Many of the features just described, especially during pitch up, are qualitatively similar to those observed in Ref. 8 in the tip vortex behind a stationary wing. However, no quantitative correspondence was observed between the stationary and oscillating vortices. In fact, the effect of wing oscillation on the flow is demonstrated quite strongly in Fig. 3 by the difference in contour shapes and magnitudes between the pitch-up and pitch-down phases of the oscillation cycle, for the same incidence, $\alpha = 10$ deg. The spiral is generally far more organized and the flow more nearly axisymmetric for the most part during the pitch-up motion than during the pitch-down motion. This difference is primarily because during the pitch-up motion the boundary layer over the inboard regions of the wing tends to remain attached to the surface resulting in a wake that is less turbulent and better organized. This organized vortical layer rolls up into the tip vortex resulting in a correspondingly well-organized vortex. On the other hand, the flow over the wing during the pitch-down motion is likely to detach itself from the surface at the larger values of α and reattach at smaller values. This results in a more turbulent and disorganized wake that rolls into the tip vortex, as can be seen from the results for $\alpha = 10$ deg, pitch down. The process involving flow attachment, detachment, and reattachment is dependent on Reynolds number (primarily via its effects on transition/relaminarization) and the oscillation parameters, namely, the reduced frequency and amplitude. This process, which also depends on whether the angle of incidence is increasing or decreasing, produces concomitant hysteresis effects on circulation and lift production. These changes propagate into the wing wake and into the tip vortex as the shear layer rolls up in the tip region. These changes do not, however, manifest themselves immediately at a given measuring station downstream. This is because of the time required for the effects to be convected from the originating regions to the measurement location. Thus, there is a phase shift in the flow properties from one station to another along the wake. One normally expects that at low Strouhal numbers ($Sr \ll 1$), the vortex behavior is quasisteady, i.e., that vortex properties at a given incidence would be the same during the pitch-up and the pitch-down parts of the oscillation cycle and would, in each case, be identical to those for a stationary tip vortex at the same wake location. However, hysteresis and phase shift are the two important causes for the vortex behind an oscillating wing to deviate from such a behavior. This departure

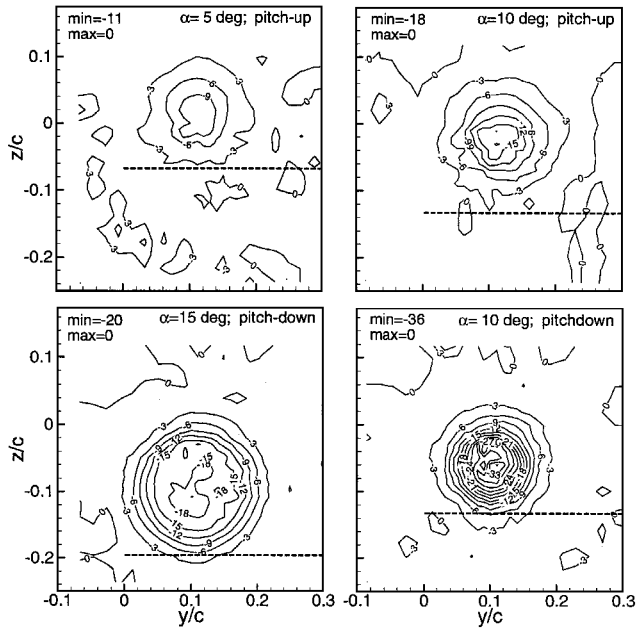

Fig. 4 Contours of nondimensional, phase-locked, axial vorticity $\omega_x c/U_\infty$ at different instantaneous incidences during the oscillation cycle at $x/c = 1.33$: Dashed line indicates the instantaneous position of the trailing edge.

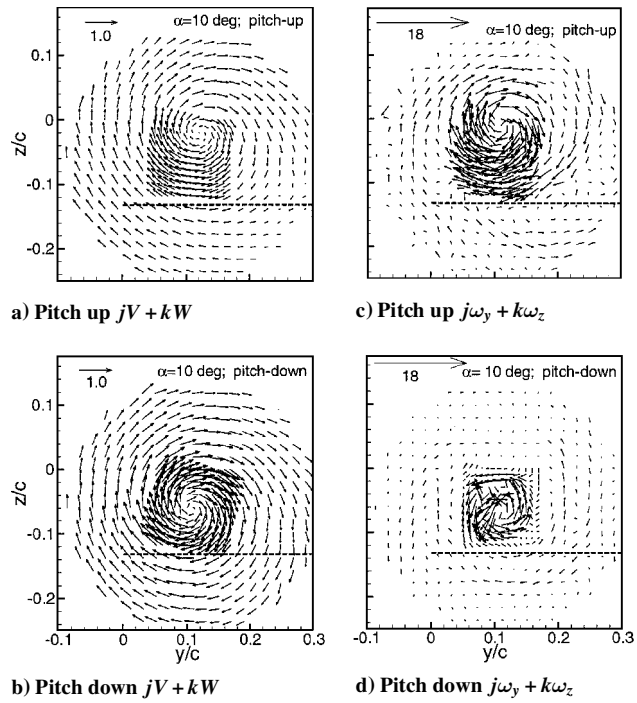

Fig. 5 Nondimensional phase-locked velocity and vorticity vectors in the cross-stream plane at $\alpha = 10$ deg and $x/c = 1.33$; reference vectors of magnitude 1 and 18 correspond to the freestream velocity and maximum axial vorticity (during pitch up), respectively: Dashed line indicates the instantaneous position of the trailing edge.

from quasisteady behavior is, indeed, observed in all of the vortex properties discussed in the following sections.

Contours of the nondimensional axial vorticity component $\omega_x c/U_\infty$ are shown in Fig. 4. These contours correspond to the same instantaneous incidences as in Fig. 3. It was observed that in all cases, the axial vorticity decayed from its peak magnitude at the vortex center to a magnitude less than 15% of this value within a radius of the order of $0.1c$. The vorticity distribution across this region, which is a result of viscous and/or turbulent diffusion, varies considerably during the oscillation cycle. The strongest (negative) vorticity (with a magnitude ranging from 11 to 36 vorticity units depending on the instantaneous incidence during the oscillation cycle) is observed near the center of the vortex. The magnitude of this vorticity is generally higher during the pitch-down motion. The difference in the size and strength of the vorticity field between the pitch-up and pitch-down phases is seen typically from the results at 10-deg incidence. The shapes of the vorticity contours do not, at first glance, give any strong indication of the disturbed state of the flow during the pitch-down part of the cycle. More careful examination of the contours showed, however, that the vorticity inside the vortex core reaches the highest negative value (of about 36 units) at 10 deg during pitch down (the case shown in Fig. 4), when the longitudinal mean velocity has the most jetlike distribution. Finally, although the vorticity field is not quite axisymmetric at this station, it is still close enough to being axisymmetric, during the entire oscillation cycle, that it is at least meaningful to extract circumferentially averaged properties from the experimental results.

Velocity and Vorticity Vectors in the Cross-Stream Plane

The nondimensional phase-locked velocity vectors $[(jV + kW)/U_\infty]$ in the cross-stream plane for $x/c = 1.33$ and $\alpha = 10$ deg are shown in Figs. 5a (pitch up) and 5b (pitch down). The length of the arrows in these plots shows the magnitude of the cross-stream velocity. The reference velocity vector shown at the top-left-hand curve in each plot denotes the magnitude (=1) of the freestream velocity. Once again, differences can be observed clearly between the results for pitch-up and pitch-down motions. It is also seen that the magnitude of the cross-stream velocity vectors is of the order of U_∞ and is, therefore, quite significant. It is also important to note that, whereas the longitudinal velocity distribution across the vortex varies drastically from a wakelike to a jetlike behavior during the oscillation cycle, there are no such trend changes that can easily be discerned in the cross-stream flow. In fact, Fig. 5b gives no strong clue to the highly agitated state of the flow at this instant, which was indicated in Fig. 3.

As the shear layer from the inboard regions of the wing surface rolls up into the tip vortex, the spanwise vorticity carried by it rotates into the axial direction and augments the axial vorticity of the tip vortex. This is seen from Figs. 5c and 5d, which show the cross-stream vorticity vectors $(j\omega_y + k\omega_z)$ normalized by U_∞/c. The cross-stream vorticity has the largest magnitude in the shear layer, which is rolling up, and is small elsewhere including the central part of the vortex, where the vorticity vector has almost aligned itself in the axial direction. The reference vectors shown at the top in Figs. 5c and 5d have a magnitude of 18 vorticity units, which is the magnitude of the axial vorticity at the center of the vortex at 10-deg incidence during pitch up (see Fig. 4). It is seen from Figs. 5c and 5d that, at this measuring station, the cross-stream vorticity is small but still significant (15–20%) compared to the streamwise vorticity. The process is once again seen to be nonquasisteady from a comparison of Fig. 5c with Fig. 5d. It is also seen that for the 10-deg pitch-down case, the data are noisy, which is the result of the agitated longitudinal mean velocity field from which the vorticity field is derived. Note also that the cross-stream vorticity vectors in Fig. 5d are generally opposite in direction to the vectors in Fig. 5c. This is largely a consequence of the difference in nature (wakelike vs jetlike) of the longitudinal mean velocity field within the vortex at these two instants and is, thus, indicative of flow agitation and separation.

Vorticity distributions in the vortex at other longitudinal locations are not shown here for lack of space. They are available from Zheng and Ramaprian.[11] Data from more downstream stations were essentially similar to those at $x/c = 1.33$, except for a gradual improvement in axisymmetry and reduction in the relative magnitude of the vorticity in the cross-stream plane. Data at smaller distances from the trailing edge, for example, at $x/c = 0.33$, indicated that the vortex is significantly nonaxisymmetric. In fact, at this station, two or more substructures were observed within the vortex during some parts of the cycle. Also, the magnitudes of vorticity were found to be generally slightly smaller at the upstream station. The spiral shear layer carrying predominantly cross-stream vorticity was more clearly identifiable at all instants during the oscillation cycle at this station. The data at this station also showed a close correspondence between vorticity modulation and instantaneous incidence. This is

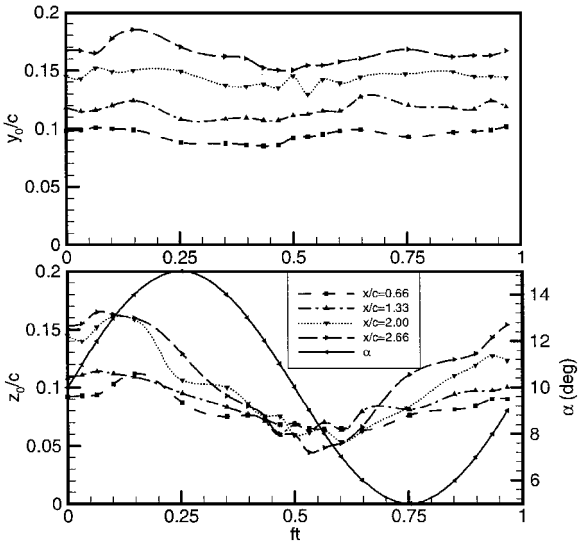

Fig. 6 Movement of the vortex center relative to the wing tip at the trailing edge during the oscillation cycle.

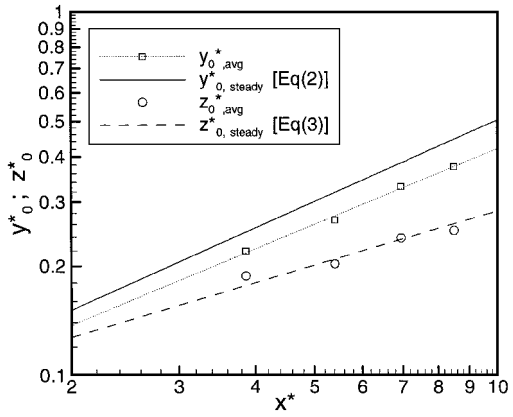

Fig. 7 Comparison of the mean vortex trajectory with the near-field correlations of Ref. 8 for a stationary wing tip vortex.

to be expected because time lag effects are relatively small at this small distance from the trailing edge.

Vortex Trajectory

The cross-stream velocity vector field exhibited relatively little scatter at all locations and at all incidences, as seen from the typical results shown in Figs. 5a and 5b. It became possible, therefore, to locate the center of the vortex with reasonable accuracy (within $\pm 0.003c$) from linear interpolations of plots, such as those shown in Fig. 5. Figure 6 shows the excursion of the vortex center as a nondimensional function of time during the oscillation cycle at four different longitudinal locations in the near field, in terms of its position (y_0, z_0) relative to the instantaneous location of the wing tip at the trailing edge. The variation of the angle of incidence is also shown in Fig. 6. It is immediately seen that the spanwise location of the vortex center y_0 moves gradually inboard with increasing distance downstream but at a given station is somewhat weakly modulated during the oscillation cycle. On the other hand, the vertical location z_0 shows significant periodic modulation. The modulation shows harmonic distortion from the sine wave at the oscillation frequency.

It was shown in Ref. 8 that, in the near field behind a stationary wing, the y and z displacements of the vortex center relative to the wing tip at the trailing edge could be described reasonably well by the equations

$$y_0/L = 0.09(x_v/L)^{0.75} \tag{2}$$

and

$$z_0/L = 0.09(x_v/L)^{0.5} \tag{3}$$

where x_v is the downstream distance measured from the leading-edge plane of the wing, which can be considered to be the approximate virtual origin plane for the vortex. The reference length scale L depends on the wing loading and was defined in Ref. 8 as $(cC_L/2)$, where C_L is the overall coefficient of lift generated by the rectangular wing. Unfortunately, phase-locked values of C_L are not available for the present operating conditions of this wing. However, using the same value of L as that found for the stationary wing at the mean angle of incidence of 10 deg, as the reference length scale, one can obtain nondimensional values y_0^* and z_0^* of the average displacements of the vortex center during the oscillation cycle. It is important to keep in mind that in the case of finite wings oscillating in pitch, due to hysteresis effects, C_L varies in a nonlinear and nonquasisteady manner with α. Hence, the use of steady-flow data to define the average length scale for the oscillating wing has some intrinsic limitations. Nevertheless, the results obtained for the average vortex trajectory for the oscillating wing are shown in Fig. 7 and compared with the stationary wing correlations, Eqs. (2) and (3). It is seen that the data for z_0^* agree reasonably well with the steady-state results, whereas the values of y_0^* are somewhat smaller (by about 15%) than for the stationary wing. Also, an index slightly less than 0.75 seems to be indicated for the power law. It is also to be noted (as discussed in Ref. 8) that proximity to tunnel sidewalls in the present experiment might have caused an increase of about 6% in the vortex rise (z^*).

Spatio-Temporal Evolution of the Vortex Structure in the Near Field

From the phase-locked, cross-stream velocity vectors field, one can obtain, for any given x location and for a given instant during the oscillation cycle, the distribution of the phase-locked circulation Γ around a circle of radius r about the vortex center. For this purpose, the cross-stream velocity field was first transformed into polar coordinates and then linearly interpolated to obtain the tangential components of the velocity at 30 radial intervals and at 24 angular intervals at each radius. The phase-locked circulation $\Gamma(r)$ at any radius r was then estimated by evaluating the circular integral

$$\Gamma = \oint v_\theta r \, dr \tag{4}$$

around the circle of radius r. Figures 8a and 8b show the results for the typical measurement station $x/c = 1.33$. The distributions are shown for several instantaneous incidences during both the pitch-up

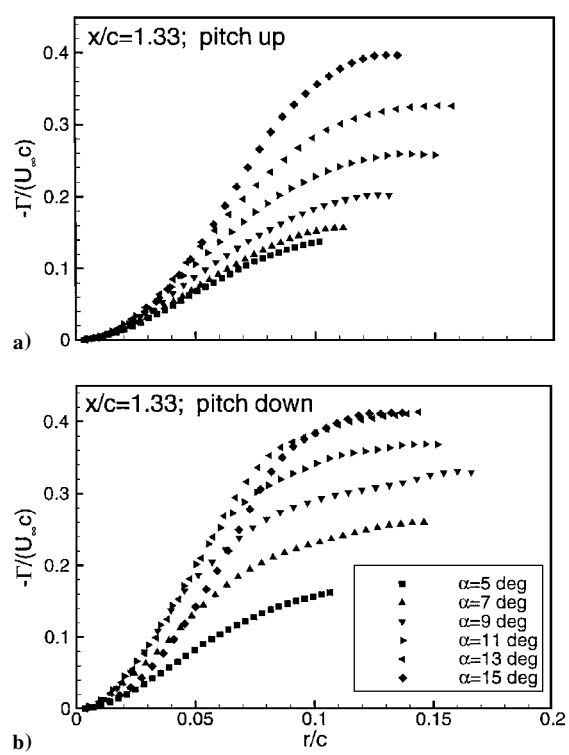

Fig. 8 Variation of phase-locked circulation with radius in the vortex.

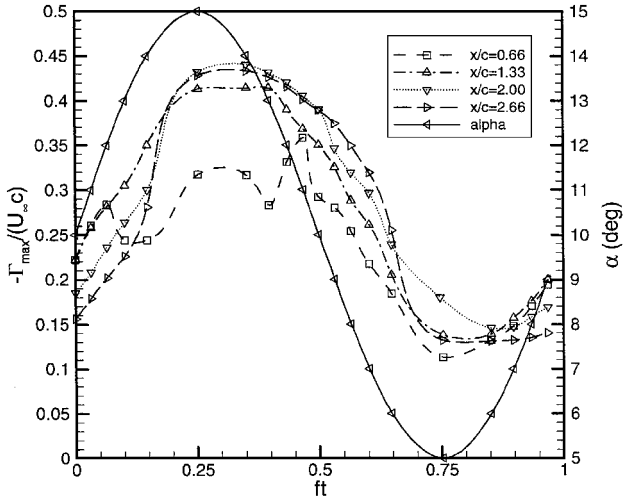

Fig. 9 Variation of maximum circulation with time in the vortex during the oscillation cycle.

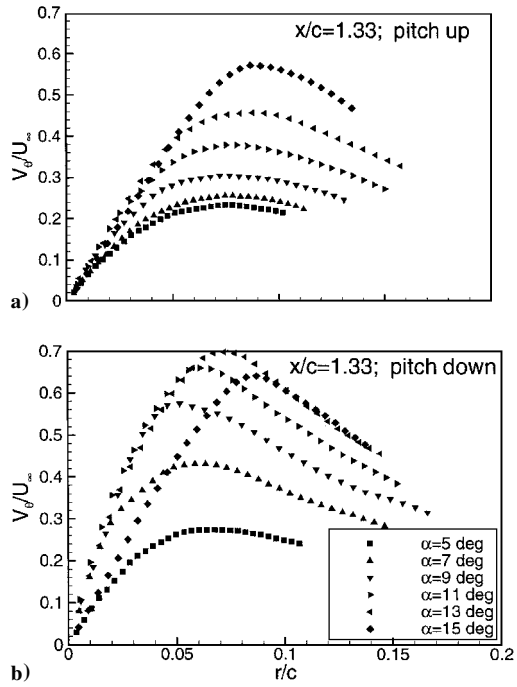

Fig. 10 Variation of circumferentially averaged, phase-locked tangential velocity with radius in the vortex.

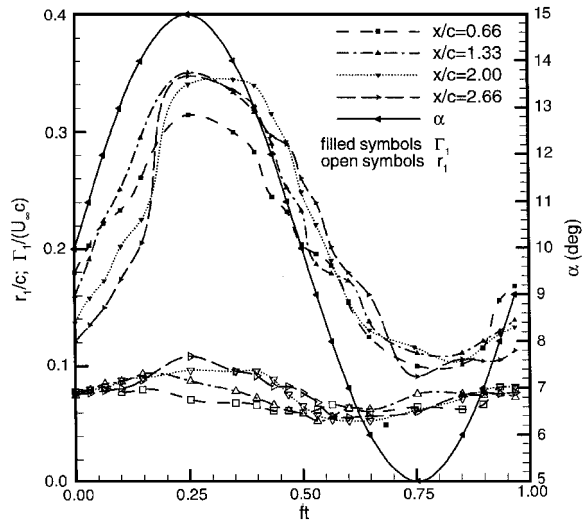

Fig. 11 Variation of the length and circulation scales of the vortex during the oscillation cycle.

and pitch-down phases of the oscillation cycle. The observed gradual and monotonic increase in circulation with radial distance is very similar to the behavior observed in Ref. 8 for a stationary vortex and is clearly indicative of the viscous/turbulent nature of the vortex. It is seen, however, that the circulation distribution varies considerably during the oscillation cycle and that the individual distributions for a given incidence during pitch-up and pitch-down motions do not correspond with each other. It is also seen that the distributions during pitch-down are somewhat distorted in shape compared to those during pitch-up.

It is reasonable to assume that the value of Γ measured at the outermost radial location corresponds to the circulation Γ_{max} associated with the tip vortex at each instantaneous incidence. Figure 9 shows the variation of Γ_{max} with time during the oscillation cycle at different downstream stations in the near field. It is seen that, except at the most upstream station $x/c = 0.66$, where the flow has not yet recovered from the disturbances created by possible flow separation and reattachment over the wing surface and also where the vortex rollup is still quite incomplete, the distributions are quite smooth. The distributions, however, show strong departures from sinusoidal behavior. For example, it is clear that during a large part of the pitch-down motion ($0.25 < ft < 0.6$) the circulation either remains constant or decreases slowly, whereas in the final part of the pitch-down, motion ($0.6 < ft < 0.75$), it decreases rapidly. Likewise, the recovery in circulation is slow in the initial part of pitch up and relatively faster over the final part. This is due to nonlinearity and hysteresis in the lift production process. In fact, the observed modulation of circulation seems to be qualitatively consistent with the modulation in lift observed in another experiment of ours on the oscillating wing.[12] Unfortunately, the oscillation conditions in the two experiments were different and, hence, quantitative comparisons are not meaningful.

The maximum magnitudes of Γ also show a small but consistent variation with distance downstream. These small changes are due to the continued rollup of the shear layer, bringing with it a small amount of additional axial vorticity into the vortex. It is also possible to detect a small but continuous increase in the delay of the occurrence of the maximum circulation relative to the instant of maximum incidence. This is caused by longitudinal convection. Because of the harmonic distortion exhibited by these distributions, it is not, however, very useful to introduce the concept of phase delay.

It was mentioned earlier that at larger distances downstream the vortex is sufficiently close to axisymmetry that it is reasonable to estimate the circumferentially averaged properties of the vortex. Figures 10a and 10b show some typical distributions of the circumferentially averaged tangential velocity across the vortex. The velocity $V_\theta(r)$ shown is phase locked and is averaged over 24 points around a circle of radius r. The distributions exhibit a maximum and qualitatively resemble those observed in a classical steady viscous trailing vortex[13] in the far field, in which the axial velocity defect $(U_\infty - U) \ll U_\infty$. The approach of the wing tip vortex in the near field of a stationary wing, toward such an asymptotic structure was studied in Ref. 8. It is now proposed to examine the oscillating wing tip vortex in the same light.

Following the approach used in earlier studies, we assume the length and circulation scales in the vortex to be provided, respectively, by the distance r_1 at which V_θ reaches a maximum in Fig. 10 and the circulation Γ_1 at r_1 as obtained from Fig. 8. Figure 11 shows the variations of these scales during the oscillation cycle at different downstream locations, including the fairly upstream station $x/c = 0.66$, where the flow shows significant asymmetry. Both scales exhibit temporal as well as spatial variations. The temporal variations are quite strong in the case of Γ_1. They are much smaller but still significant in the case of r_1. The distributions in both cases exhibit harmonic distortions primarily because of nonlinear effects associated with lift production and, to a lesser extent, due to lack of axisymmetry.

Figure 12 shows the distributions of the circulation across the vortex, plotted in semilogarithmic coordinates after normalizing the variables with the length and circulation scales defined

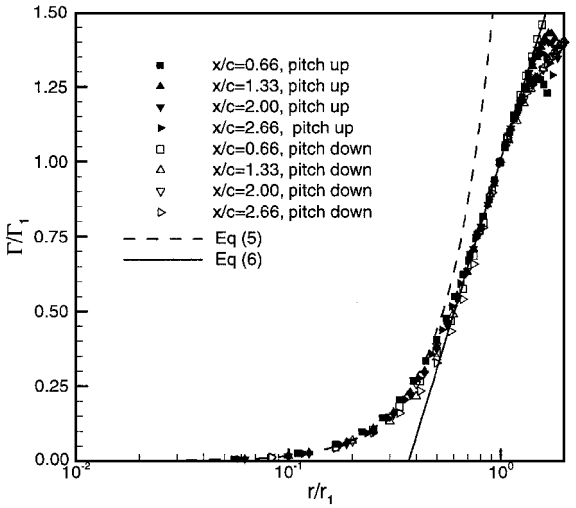

Fig. 12 Semilogarithmic plot of Γ/Γ_1 vs r/r_1 for $\alpha = 10$ deg at different downstream locations.

earlier. Typical results for a number of stations in the range $0.66 < x/c < 2.66$ are shown. Data are shown only for a fixed angle of incidence of 10 deg for the sake of clarity. It is interesting to note that the distributions exhibit self-similarity in the inner region represented by $0 < r/r_1 < 1.4$. This is true of data even from $x/c = 0.66$, where the flow has a significant level of asymmetry. Even more interestingly, this self-similar distribution was found to coincide with the corresponding distribution observed in the tip vortex behind a stationary wing in Ref. 8. It was shown in Ref. 8 that this self-similar distribution, indeed, also coincides with the universal distribution in the inner region of asymptotic viscous and turbulent vortices obtained analytically,[13,14] as well as empirically,[15] by earlier investigators. As an example, Fig. 12 shows two piecewise expressions:

$$\Gamma/\Gamma_1 = 1.74(r/r_1)^2 \tag{5}$$

$$\Gamma/\Gamma_1 = \ell n(r/r_1) + 1.0 \tag{6}$$

that were found to describe very well the inner ($r/r_1 < 0.4$) and outer ($0.6 < r/r_1 < 1.4$) parts of the core, respectively, of a stationary tip vortex in Ref. 8. Equations (5) and (6) are also in close agreement with the empirical relations suggested in Hoffman and Joubert[15] for asymptotic trailing vortices with constant eddy viscosity. Furthermore, circulation distributions at all incidences during the oscillation cycle (not shown here for the sake of clarity) were also found to collapse on the data shown in Fig. 12, in the region $r/r_1 < 1.4$. Thus, even though the vortex scales in the near field vary in a complex manner both in time and space, the core region of the vortex seems to retain essentially a universal structure during this evolution.

Conclusions

Comprehensive nonintrusive measurements have been made to explore the unsteady velocity and vorticity field associated with the evolving tip vortex in the near field of a rectangular wing oscillating in pitch. The data obtained indicate that a substantial part of the shear layer rollup and gathering of axial vorticity in the wing tip vortex occurs within a distance of about 1–2 chord lengths downstream of the trailing edge. Also, as observed in earlier studies of stationary wing tip vortices, the tip vortex becomes acceptably axisymmetric beyond this distance. The vortex center at any given x location oscillates relative to the trailing edge with significant amplitude and with some harmonic distortion. However, the average trajectory of the vortex in the near field seems to be still approximately described by the same power law correlations as are applicable to a stationary wing at the same mean incidence. The phase-locked circulation distribution across the vortex at all instants during the oscillation cycle resembles qualitatively those in a stationary vortex. Everywhere in the near field, the length and circulation scales of the vortex as well as the maximum circulation associated with it display significant harmonic distortion in their variation during the oscillation cycle. However, beyond about 0.7 chordlength in the wake, the normalized circulation exhibits the same universal structure as observed in steady flow, over most of the core region of the vortex at all instants during the oscillation cycle and at all locations in the near wake.

Acknowledgments

This work was performed under support from U.S. Army Research Office Grants DAAL03-87-G-0011 and DAAL03-91-G-0026 and U.S. Air Force Office of Scientific Research Grant AFOSR-90-0131. The support from these sources is gratefully acknowledged.

References

[1]Freymuth, P., "Further Visualization of Combined Wing-Tip and Starting Vortex," *AIAA Journal*, Vol. 25, No. 9, 1987, pp. 1153–1159.

[2]Freymuth, P., Finaish, F., and Bank, W., "Visualization of Wing-Tip Vortices in Accelerating and Steady Flow," *Journal of Aircraft*, Vol. 23, No. 9, 1985, pp. 730–733.

[3]Freymuth, P., Finaish, F., and Bank, W., "The Wing-Tip Vortex System in a Starting Flow," *Zeitschrift fur Flugwissenschaften und Weltraumforscung*, Vol. 10, No. 2, 1986, pp. 116–118.

[4]Chigier, N. A., and Corsiglia, V. R., "Tip Vortices—Velocity Distributions," NASA TM-X-62087, Sept. 1971.

[5]Corsiglia, V. R., Schwind, R. K., and Chigier, N. A., "Rapid Scanning Three Dimensional Hot Wire Anemometer Surveys of Wing-Tip Vortices," *Journal of Aircraft*, Vol. 10, No. 12, 1973, pp. 752–757.

[6]Francis, M. S., and Kennedy, D. A., "Formation of a Trailing Vortex," *Journal of Aircraft*, Vol. 16, No. 3, 1979, pp. 148–154.

[7]McAlister, K. W., and Takahashi, R. K., "Wing Pressure and Trailing Vortex Measurements," AVSCOM TR 91-1-003, NASA TP 3151, Nov. 1991.

[8]Ramaprian, B. R., and Zheng, Y., "Measurements in the Roll-Up Region of the Tip Vortex from a Rectangular Wing," *AIAA Journal*, Vol. 35, No. 12, 1997, pp. 1837–1843.

[9]Dacles-Mariani, J., Zilliac, G. G., Chow, J. S., and Bradshaw, P., "Numerical/Experimental Study of a Wingtip Vortex in the Near Field," *AIAA Journal*, Vol. 33, No. 9, 1995, pp. 1561–1569.

[10]Chow, J. S., Zilliac, G. G., and Bradshaw, P., "Mean and Turbulence Measurements in the Near Field of a Wingtip Vortex," *AIAA Journal*, Vol. 35, No. 10, 1997, pp. 1561–1567.

[11]Zheng, Y., and Ramaprian, B. R., "An Experimental Study of the Wing Tip Vortex in the Near Wake of a Rectangular Wing," Dept. of Mechanical Engineering, Rept. MME-TF-93-1, Washington State Univ., Pullman, WA, June 1993.

[12]Szafruga, S., and Ramaprian, B. R., "Pressure Measurements over the Tip Region of a Rectangular Wing—Part II. Oscillating Wing," AIAA Paper 94-1949, June 1994.

[13]Batchelor, G. K., "Axial Flow in Trailing Vortices," *Journal of Fluid Mechanics*, Vol. 20, Pt. 4, Dec. 1964, pp. 645–658.

[14]Squire, H. B., "The Growth of a Vortex in Turbulent Flow," *Aeronautical Quarterly*, Vol. 16, 1965, pp. 302–306.

[15]Hoffman, E. R., and Joubert, P. N., "Turbulent Line Vortices," *Journal of Fluid Mechanics*, Vol. 16, Pt. 3, July 1963, pp. 395–411.

A. Plotkin
Associate Editor